Supporting Information for

Ascorbic Acid-Induced Fiber-Scrolling of Titanium Carbide $Ti_3C_2T_x$ MXene

*Jinxin Cao,[a] Yuru Wang,[a] Bingqing Wei,[b] Jiaxin Ye [c] and Qing Zhang *[a]*

[a.] Institutes of Physical Science and Information Technology, Anhui University, Hefei 230039, Anhui, China

[b.] Department of Mechanical Engineering, University of Delaware, Newark, Delaware 19716, USA

[c.] School of Mechanical Engineering, Hefei University of Technology, Hefei 230009, Anhui, China

*E-mail: zhangq@ahu.edu.cn

Supplementary Materials:
Figures S1-S12
Tables S1-S5

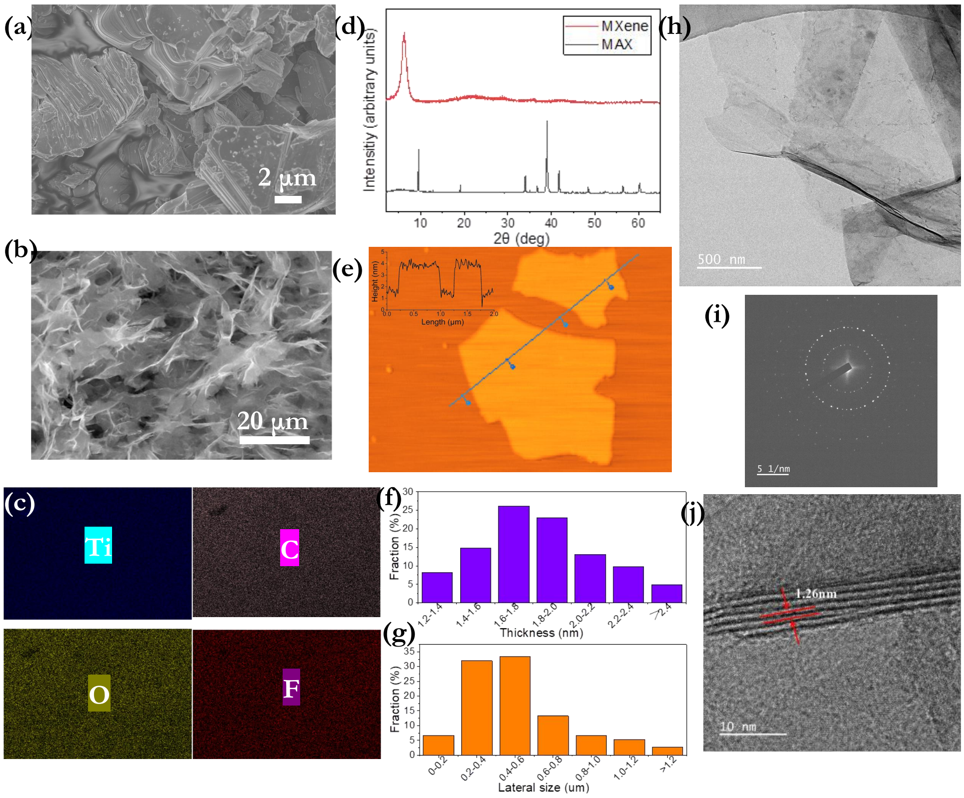

Figure S1. SEM of (a) MAX, (b) as-synthesized $Ti_3C_2T_x$ MXene and (c) the corresponding EDS mapping; (d) XRD of MAX and the $Ti_3C_2T_x$ MXene; (e) AFM image of the $Ti_3C_2T_x$ MXene deposited on mica with height profile along with the blue line; (f) Thickness distribution and (g) lateral size distribution of the $Ti_3C_2T_x$ MXene for 65 platelets; (h) TEM image, (i) electron diffraction pattern and (j) HR-TEM image of the $Ti_3C_2T_x$ MXene.

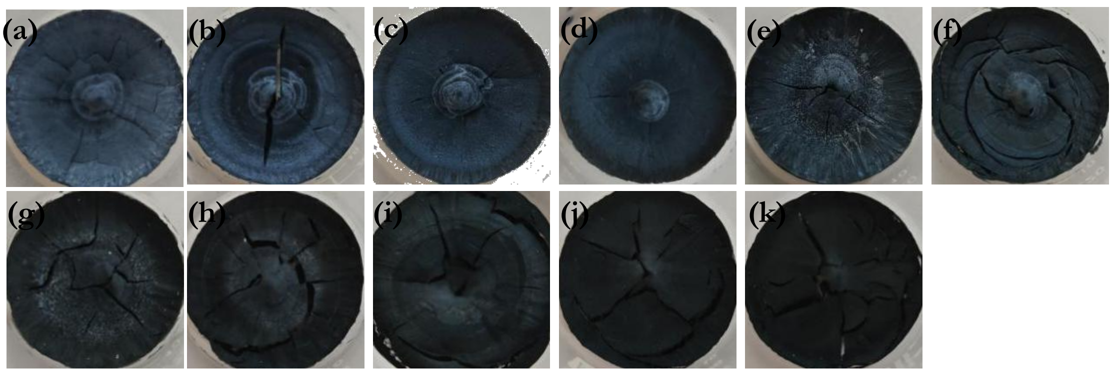

Figure S2. The optical photographs of M_xAA_y: As increasing the AA ratio (x:y = 10:0, 10:1, 10:2, 10:4, 10:6, 10:8, 10:10, 10:15, 10:17, 10:20, 10:25), the obtained samples presented "soft to less-soft" texture and gradually darkening color.

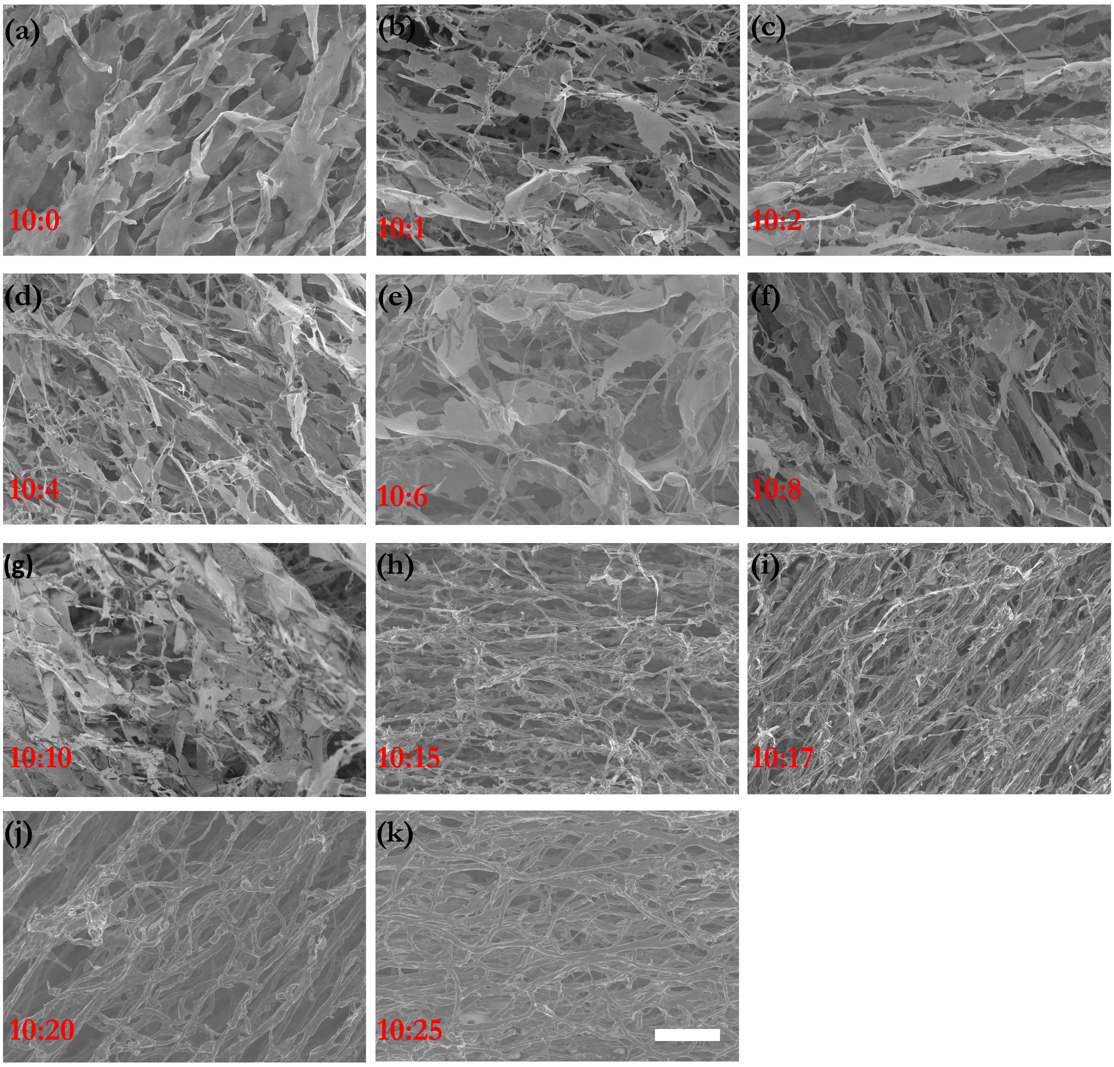

Figure S3. The SEM images of M_xAA_y (scale bar: 20 μm): Comparing the structures of 10:1, 10:2, and 10:4, besides the emergence of fibers, there is also an increase of the aspect ratio and the MXene flakes turns to long-strip shaped. In addition, it was worth noting that the length of a single fiber can reach tens or even hundreds of microns.

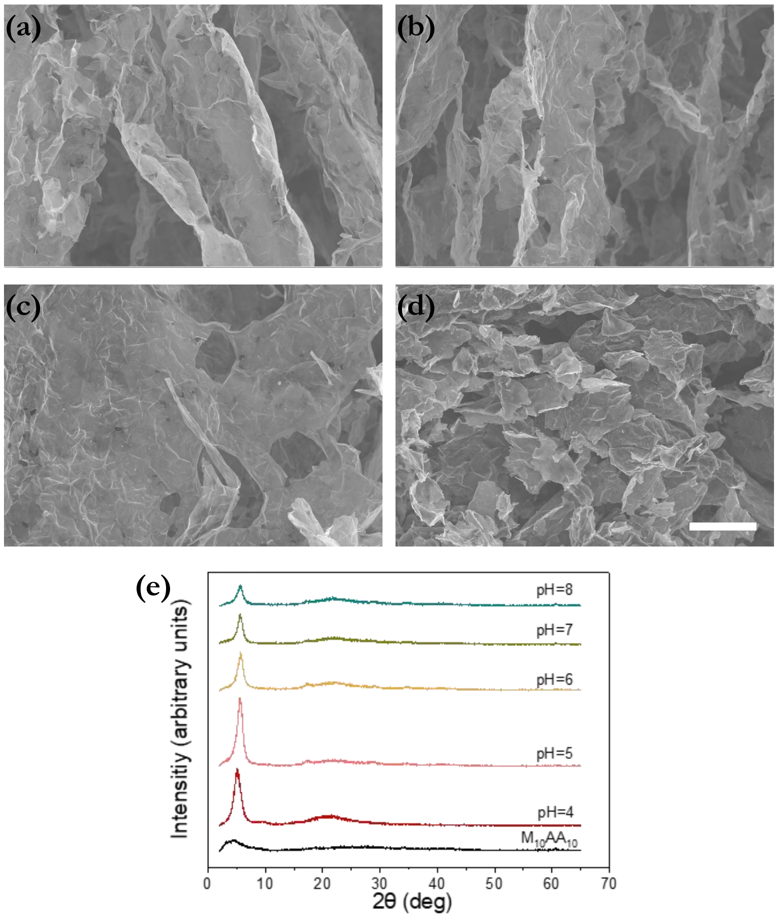

Figure S4. SEM images of $M_{10}AA_{10}$ treated with $NaHCO_3$: (a) to pH = 5, (b) to pH = 6, (c) to pH = 7, and (d) to pH = 8; and the correspondng XRD results. (scale bar: 4 μm).

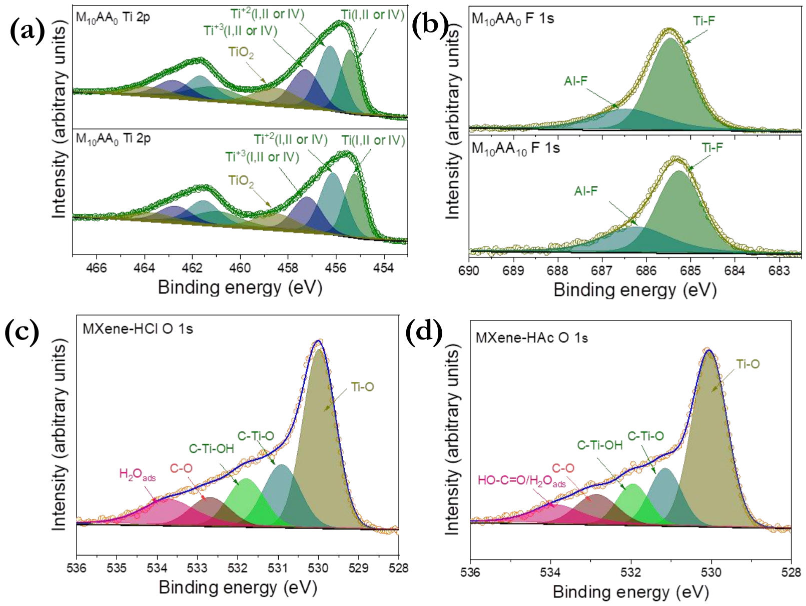

Figure S5. High-resolution XPS spectra: (a) Ti 2p and (b) F 1s of MXene ($M_{10}AA_0$) and $M_{10}AA_{10}$; O 1s of MXene treated with HCl (c) and of MXene treated with HAc (d).

Table S1. XPS fitting results for $M_{10}AA_0$ and $M_{10}AA_{10}$.

Peak($M_{10}AA_0$)	**Position(eV)**	**Area(%)**	**Peak($M_{10}AA_{10}$)**	**Position(eV)**	**Area(%)**
Ti (I,II or IV) [a)]	455.412 (461.127)	27.30	Ti (I,II or IV)	455.212 (460.903)	29.30
Ti^{+2} (I,II or IV)	456.229 (461.651)	34.70	Ti^{+2} (I,II or IV)	456.106 (461.508)	35.42
Ti^{+3} (I,II or IV)	457.272 (462.772)	23.19	Ti^{+3} (I,II or IV)	457.189 (462.693)	21.70
TiO_2	458.528 (463.920)	14.82	TiO_2	458.512 (463.806)	13.58
C-Ti	282.217	42.87	C-Ti	281.990	15.07
C-Ti-O	283.008	11.52	C-Ti-O	282.945	5.71
sp^2 C	284.807	33.19	sp^2 C	284.834	14.00
C-O	286.287	12.42	C-O	286.377	28.75
			C-O-Ti	**286.949**	**21.96**
			O-C=O	288.683	11.57
			C-F	291.931	2.94
Ti-O	530.159	51.62	Ti-O	529.969	10.09
C-Ti-O	531.123	15.80	C-Ti-O	530.759	1.67
C-Ti-OH	531.970	12.39	**C-O-Ti**	**531.522**	**5.40**
C-O	532.813	10.70	C-Ti-OH	532.231	13.01
H_2O_{ads}	533.889	9.49	C-O	533.105	38.18
			O-C=O/H_2O_{ads}	533.810	31.65
Ti-F	685.459	71.11	Ti-F	685.251	64.47
Al-F	686.455	28.89	Al-F	686.219	35.53

Table S2. XPS fitting results for MXene treated with HCl and HAc.

Peak(HCl)	**Position(eV)**	**Area(%)**	**Peak(HAc)**	**Position(eV)**	**Area(%)**
Ti (I,II or IV)[a)]	455.350 (461.100)	31.62	Ti (I,II or IV)	455.380 (461.134)	35.41
Ti^{+2} (I,II or IV)	456.230 (461.650)	29.39	Ti^{+2} (I,II or IV)	456.240 (461.621)	22.41
Ti^{+3} (I,II or IV)	457.270 (462.770)	18.00	Ti^{+3} (I,II or IV)	457.111 (462.862)	23.91
TiO_2	458.528 (463.920)	20.98	TiO_2	458.530 (463.926)	18.26
C-Ti	282.165	41.50	C-Ti	282.194	43.19
C-Ti-O	282.917	10.95	C-Ti-O	283.049	7.65
sp^2 C	284.800	30.10	sp^2 C	284.800	38.03
C-O	286.246	17.46	C-O	286.385	9.10
			O-C=O/H_2O_{ads}	289.131	2.03
Ti-O	529.972	45.72	Ti-O	530.045	51.81
C-Ti-O	530.898	17.73	C-Ti-O	531.142	15.42
C-Ti-OH	531.784	13.52	C-Ti-OH	531.946	11.08
C-O	532.681	8.81	C-O	532.856	10.32
H_2O_{ads}	533.726	14.22	O-C=O/H_2O_{ads}	533.876	11.36
Ti-F	685.207	85.61	Ti-F	685.208	77.90
Al-F	686.455	14.39	Al-F	686.326	22.10

[a)] (I refers to Ti atoms bonded to C atoms and one O atom; II refers to Ti atoms bonded to C atoms and an OH group; IV refers to Ti atoms bonded to OH terminations that physisorbed to water molecules).[42]

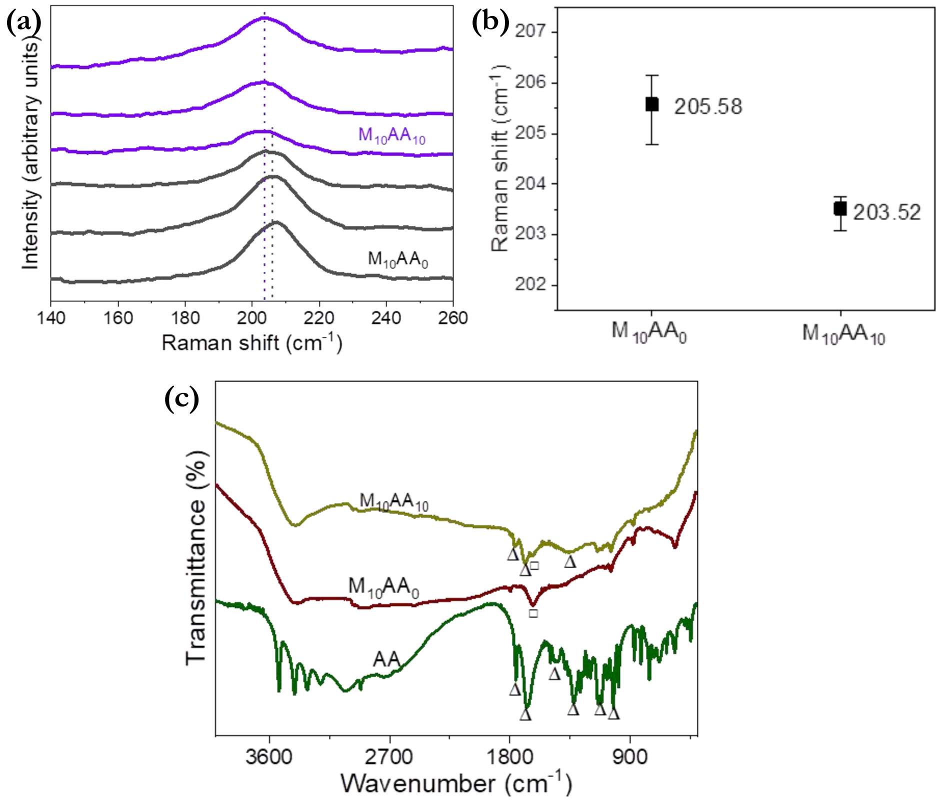

Figure S6. Raman spectra of $M_{10}AA_0$ and $M_{10}AA_{10}$: (a) ranged from 140 to 260 cm^{-1} and (b) the corresponding peak shifts as statistically derived from (a); (c) FTIR spectra of $M_{10}AA_0$ and $M_{10}AA_{10}$ and AA.

In particular, Raman results of $M_{10}AA_0$ and $M_{10}AA_{10}$ both show characteristic peaks of $Ti_3C_2T_x$ MXene (Figure 3b), where the A_{1g} mode around 204 cm^{-1} represents the overall out-of-plane vibrations of titanium atoms, carbon atoms and surface groups. The region 230-470 cm^{-1} is the E_g mode, which represents the in-plane vibrations of the surface groups attached to the titanium atoms. The region 580-730 cm^{-1} is mainly due to carbon vibrations (both the A_{1g} and E_g mode).[46]

The FTIR spectrum of pure AA admits characteristic peaks at 1757 cm^{-1} (C=O stretching), 1667 cm^{-1} (C=C stretching), 1455 cm^{-1} (C-H bending), 1320 cm^{-1} (C=C-OH), 1120 cm^{-1} (C-O-C stretching) and 1026 cm^{-1} (C-O bending).[36,49] $M_{10}AA_0$ ($Ti_3C_2T_x$) admits a characteristic peak at 1633cm^{-1} assigned to the functional group -OH on the surface of $Ti_3C_2T_x$.[36] $M_{10}AA_{10}$ shows characteristic peaks from both AA and $Ti_3C_2T_x$; moreover, two peaks at 1143 cm^{-1}, 1114 cm^{-1} located close to C-O-C stretching vibration of AA, possibly overlapped with peaks due to C-O stretching vibration of C-O-Ti bidentate complexes.[47]

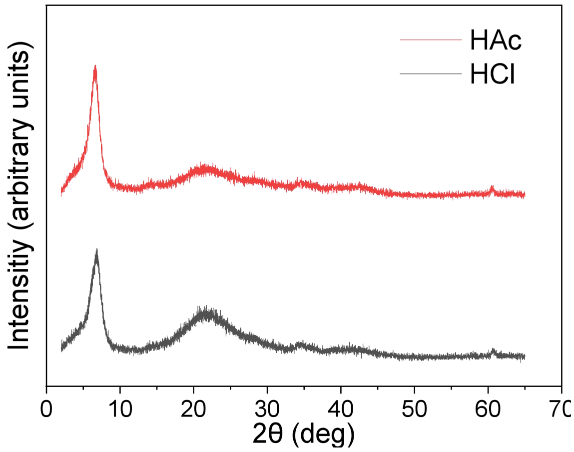

Figure S7. XRD results of MXene treated with HAc and HCl.

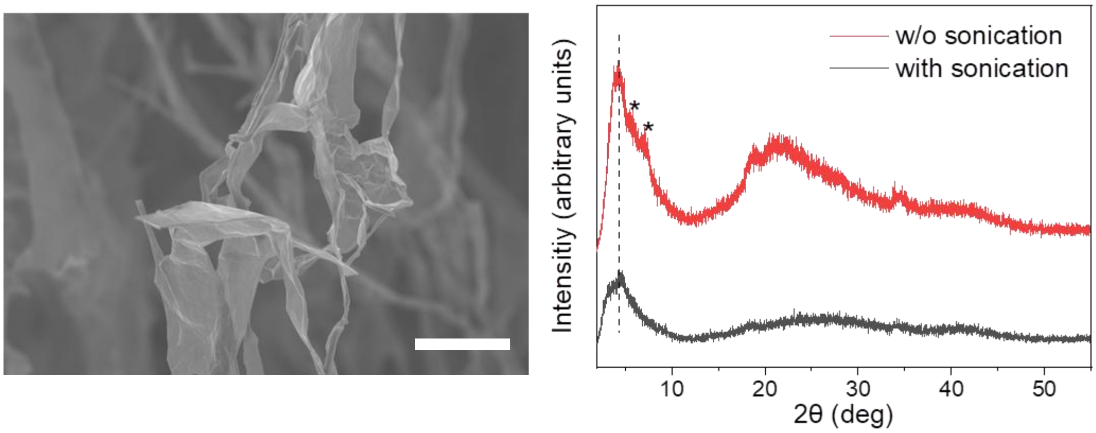

Figure S8. SEM image of MXene:AA (10:10) without sonication treatment and XRD results of MXene:AA (10:10) with and without sonication treatment (Scale bar: 4 μm).

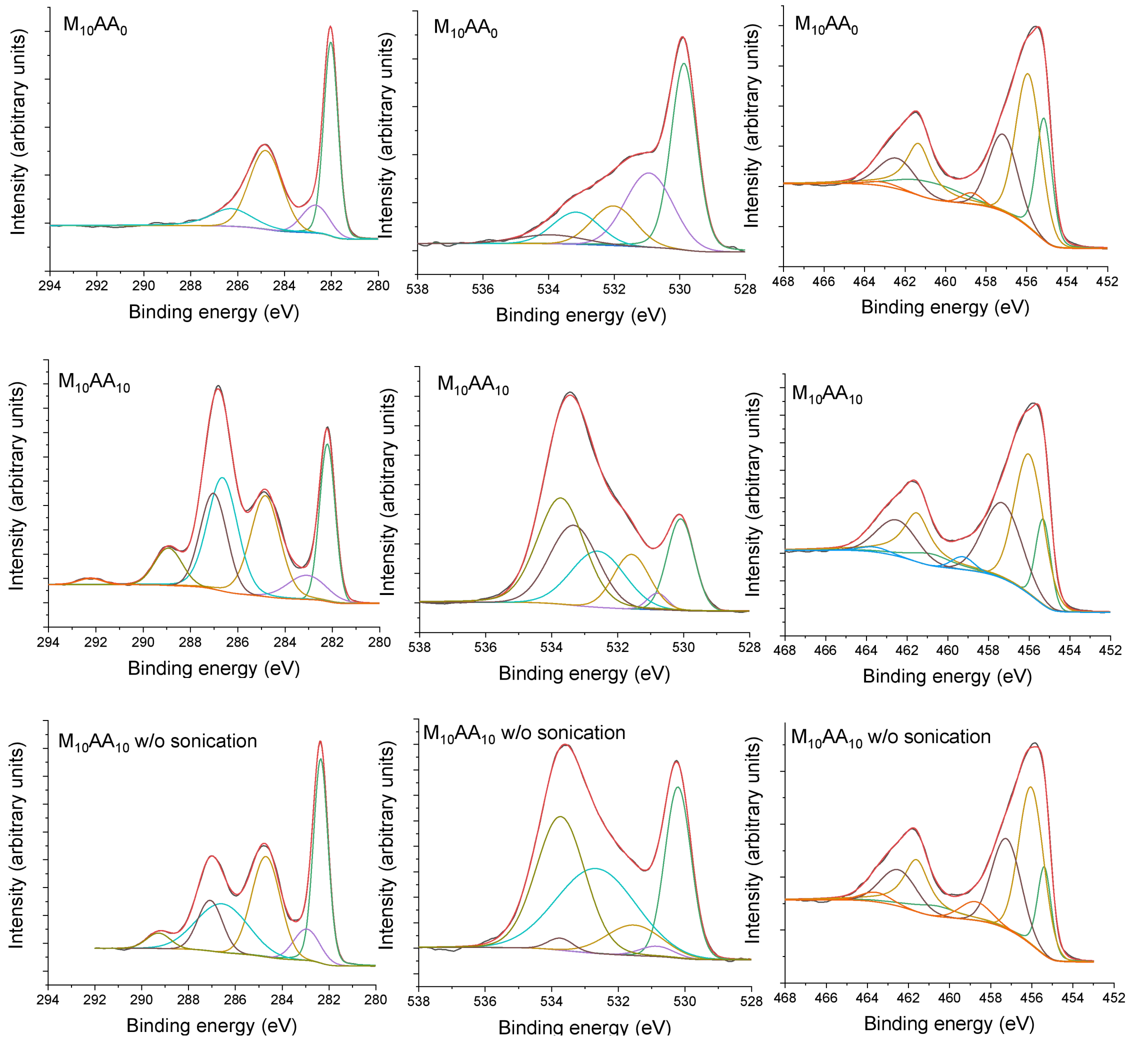

Figure S9. High-resolution XPS spectra: C 1s, O 1s and Ti 2p of MXene ($M_{10}AA_0$), $M_{10}AA_{10}$ and $M_{10}AA_{10}$ without sonication treatment.

Table S3. XPS fitting results for $M_{10}AA_0$, $M_{10}AA_{10}$ and $M_{10}AA_{10}$ without sonication treatment.

Peak ($M_{10}AA_0$)	Position (eV)	Area (%)	Peak ($M_{10}AA_{10}$)	Position (eV)	Area (%)	Peak ($M_{10}AA_{10}$, w/o sonication)	Position (eV)	Area (%)
Ti (I,II or IV) [a)]	455.142 (460.75)	24.68	Ti (I,II or IV) [a)]	455.311 (460.835)	15.24	Ti (I,II or IV) [a)]	455.386 (460.711)	15.96
Ti^{+2} (I,II or IV)	455.916 (461.339)	46.25	Ti^{+2} (I,II or IV)	456.007 (461.516)	47.76	Ti^{+2} (I,II or IV)	456.025 (461.606)	46.42
Ti^{+3} (I,II or IV)	457.163 (462.405)	26.29	Ti^{+3} (I,II or IV)	457.305 462.498	33.70	Ti^{+3} (I,II or IV)	457.234 462.489	31.00
TiO_2	**458.709 (463.113)**	**2.77**	**TiO_2**	**459.26 463.597**	**3.30**	**TiO_2**	**458.742 463.583**	**6.62**
C-Ti	282.026	40.87	C-Ti	282.215	17.64	C-Ti	282.357	28.90
C-Ti-O	282.678	10.62	C-Ti-O	283.085	6.80	C-Ti-O	282.956	7.42
sp^2 C	284.807	35.95	sp2 C	284.838	23.05	sp2 C	284.694	26.28
C-O	286.263	12.56	C-O	286.642	25.81	C-O	286.558	22.78
			C-O-Ti	**287.024**	**18.36**	**C-O-Ti**	**287.076**	**11.30**
			O-C=O	288.931	7.31	O-C=O	289.279	3.32
			C-F	292.225	1.04			
Ti-O	529.874	41.79 (*50.03*)	Ti-O	530.091	14.52 (*31.66*)	Ti-O	530.21	22.45 (*34.35*)
C-Ti-O	530.938	27.97 (*33.48*)	C-Ti-O	530.795	1.96 (*4.27*)	C-Ti-O	530.847	1.70 (*2.61*)
C-Ti-OH	**532.019**	**13.77 (*16.49*)**	C-O-Ti	531.58	11.73 (*25.58*)	C-O-Ti	531.531	8.27 (*12.65*)
C-O	533.159	11.77	**C-Ti-OH**	**532.601**	**17.64 (*38.48*)**	**C-Ti-OH**	**532.665**	**32.92 (*50.38*)**
H_2O_{ads}	533.942	4.70	C-O	533.33	22.66	C-O	533.74	1.48
			O-C=O /H_2Oads	533.725	31.49	O-C=O /H_2Oads	533.732	33.17

*Note: In O 1s, atomic ratios given in brackets are calculated with C-O and O-C=O /H_2Oads excluded.

MXene:AA (10:10) without sonication shows different morphology (with curled scrolls, but not tightly structured fibers) from $M_{10}AA_{10}$. As shown in the above XRD results, MXene:AA (10:10) without sonication showed two peaks on the right side shoulder, indicating relatively incomplete AA intercalation as compared to $M_{10}AA_{10}$;

moreover, the broad shoulder on the left side is only observed in $M_{10}AA_{10}$, not in MXene:AA (10:10) without sonication, which means no fiber formation without sonication, consistent with the SEM results.

As shown in the Table S3, probe sonication has several effects: 1 atomic ratio of TiO_2 is slightly decreased from 6.62 at.% to 3.30 at% (Ti 2p); 2 atomic ratios of C-O-Ti are raised, from 11.30 at.% to 18.36 at.% (C 1s) and from 8.27 at.% to 11.73 at.% (O 1s); 3 atomic ratio of C-Ti-OH is reduced from 32.92 at.% to 17.64 at.% (13.77 at.% before mixing with AA). Based on the research of Gogotsi *et al.*[50],

$$\mathrm{Ti_3C_2O_x(OH)_yF_z + \delta\bar{e} + \delta H^+ \rightarrow Ti_3C_2O_{x-\delta}(OH)_{y+\delta}F_z}$$

is the electrochemical reaction possibly happening in the $Ti_3C_2T_x$ MXene. Therefore, after mixing with MXene, AA can be oxidized into dehydroascorbic acid, producing e^- and H^+, and at the same time, C-Ti-O transforms into C-Ti-OH, while probe sonication promotes the formation of C-O-Ti. Probe sonication also leads to slight reduction of MXene.

Hence, sonication treatment promotes the AA intercalation as well as the formation of C-O-Ti bonding and is indispensible for successful fiber formation.

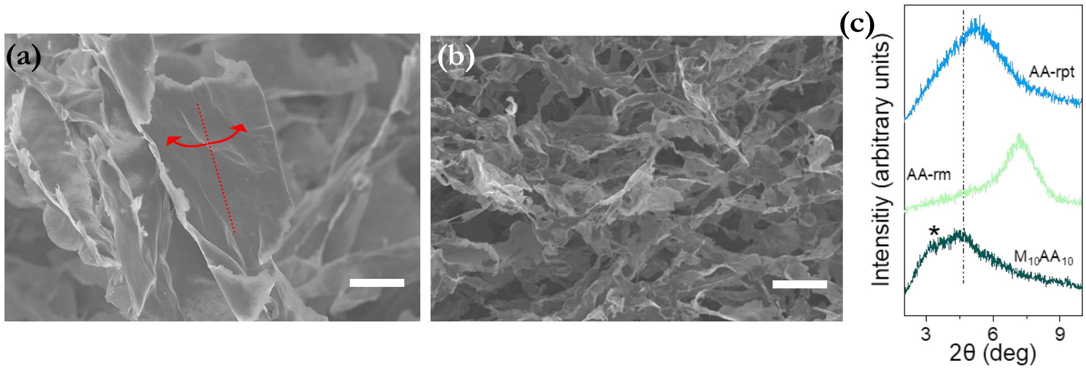

Figure S10. SEM images of (a) $M_{10}AA_{10}$ with AA removed (AA-rm) and (b) then repeating treatment with AA again (AA-rpt) and (c) their XRD results (scale bar: 10 μm).

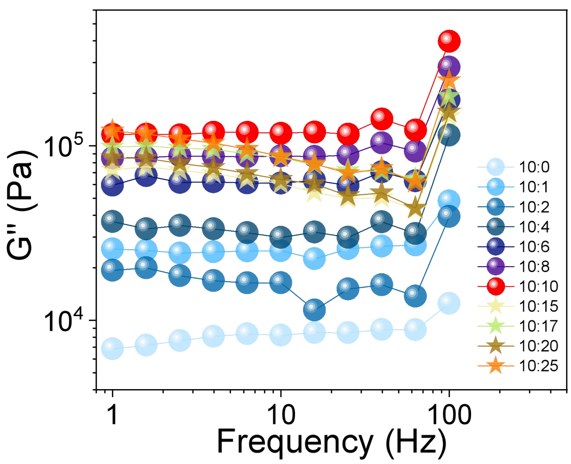

Figure S11. Loss modulus G" vs. frequency of $M_{10}AA_x$ with different AA ratios at constant stain of 0.1%.

Table S4. Thickness and aspect ratio of pressed $M_{10}AA_x$ films with different AA ratios for conductivity measurement.

Sample	Thickness (μm)	Aspect Ratio	Sample	Thickness (μm)	Aspect Ratio
$M_{10}AA_0$	5	4	$M_{10}AA_{10}$	9	2.5
$M_{10}AA_1$	5	4	$M_{10}AA_{15}$	11	2
$M_{10}AA_2$	6	3	$M_{10}AA_{17}$	14	3
$M_{10}AA_4$	10	2	$M_{10}AA_{20}$	24	2
$M_{10}AA_6$	9	3	$M_{10}AA_{25}$	22	3
$M_{10}AA_8$	8	5.7			

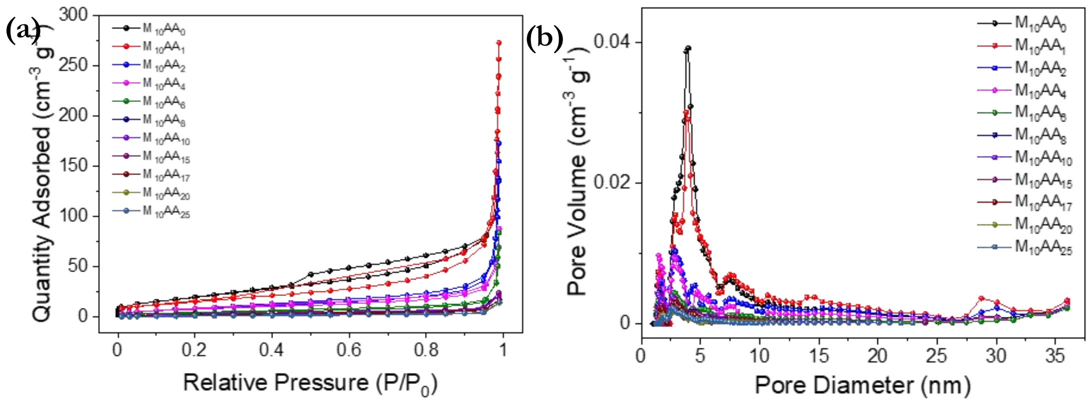

Figure S12. (a) N_2 adsorption-desorption isotherms and (b) pore size distribution curves of $M_{10}AA_x$ with different AA ratios.

Table S5. Specific surface area and average pore diameter of $M_{10}AA_x$ with different AA ratios.

Sample	Surface Area ($m^2 \cdot g^{-1}$)	Average pore diameter (nm)	Sample	Surface Area ($m^2 \cdot g^{-1}$)	Average pore diameter (nm)
$M_{10}AA_0$	76.271	3.969	$M_{10}AA_{10}$	10.633	1.475
$M_{10}AA_1$	57.733	3.794	$M_{10}AA_{15}$	8.698	2.897
$M_{10}AA_2$	32.459	2.769	$M_{10}AA_{17}$	7.912	2.769
$M_{10}AA_4$	29.859	1.475	$M_{10}AA_{20}$	4.974	2.769
$M_{10}AA_6$	15.581	2.769	$M_{10}AA_{25}$	4.263	2.647
$M_{10}AA_8$	10.431	1.475			